Metamorphosis of a quantum Hall bilayer state into a composite fermion metal

ARTICLE *in* SOLID STATE COMMUNICATIONS · FEBRUARY 2007

Impact Factor: 1.9 · DOI: 10.1016/j.ssc.2007.07.005 · Source: arXiv

7 AUTHORS, INCLUDING:

Stefano Luin
Scuola Normale Superiore di Pisa
40 PUBLICATIONS **379** CITATIONS
SEE PROFILE

Brian S. Dennis
Rutgers, The State University of New Jersey
148 PUBLICATIONS **2,164** CITATIONS
SEE PROFILE

Metamorphosis of a Quantum Hall Bilayer State into a Composite Fermion Metal

Biswajit Karmakar,[1] Stefano Luin,[1] Vittorio Pellegrini,[1] Aron Pinczuk,[2,3] Brian S. Dennis,[3] Loren N. Pfeiffer,[3] and Ken W. West[3]

[1] *NEST CNR-INFM and Scuola Normale Superiore, Piazza dei Cavalieri 7, I-56126 Pisa (Italy)*
[2] *Dept. of Appl. Phys. and Appl. Math, Dept. of Physics, Columbia University, New York, New York 10027*
[3] *Bell Laboratories, Alcatel-Lucent, Murray Hill, New Jersey 07974*

(Dated: February 6, 2008)

Composite fermion metal states emerge in quantum Hall bilayers at total Landau level filling factor ν_T=1 when the tunneling gap collapses by application of in-plane components of the external magnetic field. Evidence of this transformation is found in the continua of spin excitations observed by inelastic light scattering below the spin-wave mode at the Zeeman energy. The low-lying spin modes are interpreted as quasiparticle excitations with simultaneous changes in spin orientation and composite fermion Landau level index.

PACS numbers: 73.43.Nq, 73.21.-b, 71.35.Lk, 73.43.Lp

Distinct quantum phases of electrons exist in coupled bilayers of double quantum wells at total Landau level filling factor $\nu_T = 1$. They result from the interplay between interlayer and intralayer interactions dictated by d/l_B (d is the distance between the two layers and l_B is the magnetic length), and by Δ_{SAS}/E_c, where Δ_{SAS} is the tunnelling gap and $E_c = e^2/\varepsilon l_B$ (ε is the dielectric constant) is the intra-layer Coulomb energy [1, 2].

In the strong interlayer interaction regime, at sufficiently low d/l_B or large Δ_{SAS}/E_c, the ground states at $\nu_T = 1$ are incompressible quantum Hall (QH) fluids [2] (see Fig.1(a)). In the zero-tunneling limit, these incompressible states can be described as condensates of interlayer excitons displaying superfluid-like behavior [3, 4]. The appearance of such highly-correlated QH states occurs when the Landau levels originating from the left/right quantum-well subbands are degenerate.

Finite values of Δ_{SAS} split the quantum-well states into their symmetric and antisymmetric combinations. Mean-field approaches have described the QH physics in these regimes assuming full occupation of the lowest symmetric Landau level [5]. However, recent inelastic light scattering experiments demonstrated the breakdown of this mean-field picture by showing that even at $\Delta_{SAS} > 0$ inter-layer correlations favor spontaneous occupation of the excited antisymmetric level [6]. These correlated incompressible states can be described in terms of electron-hole excitonic pairs across Δ_{SAS} by making a particle-hole transformation in the lowest Landau level. These observations uncover a breakdown of mean-field descriptions that have linked the stability of these states to the collapse of the magneto-roton energies of the tunneling charge-density mode [5, 7].

As the interlayer interaction is reduced either by decreasing Δ_{SAS}/E_c or increasing d/l_B, the incompressible excitonic phase is replaced by compressible states as shown in Fig.1(a). The nature of these compressible states at $\nu_T = 1$ is a subject of current investigation. Several theoretical works have predicted that composite-fermion (CF) metals occur in these compressible phases [1, 3, 8]. In the limit of vanishingly small inter-layer interactions ($d/l_B \to \infty$), the compressible CF metals arise because the two layers, each at $\nu = 1/2$, are decoupled.

CFs were originally introduced to explain the hierarchy of incompressible states observed in the fractional QH regime [9]. Due to Chern-Simons gauge fields, CF's with two attached vortices experience effective magnetic fields $B^* = B \cdot (1 - 2\nu)$. As $\nu \to 1/2$ the CF level spacing vanishes and the CF's are expected to form a new type of metal with a well-defined Fermi surface.

The interplay between incompressible excitonic and compressible CF metal phases in bilayers is a topic of great current interest [3, 8, 10, 11, 12, 13, 14, 15]. On the other hand, experimental signatures revealing the impact of CF physics in bilayers at $\nu_T = 1$ have been difficult to identify. Recent combined magneto-transport and nuclear magnetic resonance studies indicate a tendency to lose spin polarization at the incompressible-to-compressible phase transition, which suggests possible links with CF liquids [16, 17].

In this letter we report inelastic light scattering spectra in the $\nu_T = 1$ electron bilayers at finite Δ_{SAS} that reveal the metamorphosis of the excitonic incompressible state into a compressible CF metal. The tunability of Δ_{SAS} with changes of the in-plane component of the magnetic field [18] is used here to go across the incompressible-compressible phase boundary. When the bilayers are in the excitonic incompressible phase we observe a sharp SW at E_z due to Larmor theorem. Below a critical value of Δ_{SAS}/E_c instead a striking continuum of excitations is seen at energies smaller than E_z.

The continuum of spin transitions seen below E_z is regarded as evidence of the filling of CF states up to the CF Fermi energy as shown in Fig.1(b). These spin modes are interpreted as spin-flip excitations (SF_{CF}) of the CF metal in which orientation of spin and CF Landau level

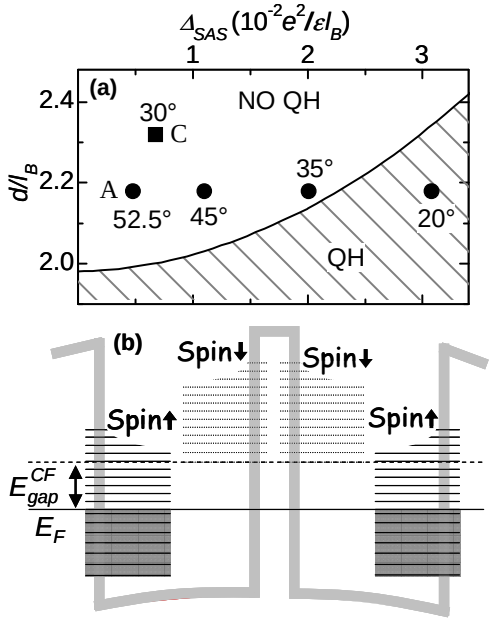

FIG. 1: (a) Phase diagram between compressible (NO QH) and incompressible (QH) phases as obtained by magneto-transport experiments [2]. Positions of samples studied in this work at different tilt angles are also shown. (b) Schematic diagram of weakly coupled composite-fermion (CF) metals in the bilayer system at $\nu_T = 1$. E_F and E_{gap}^{CF} are the Fermi energy and spin-flip energy gap of the CF metal, respectively.

number change simultaneously [19] as displayed in the bottom-right panel of Fig.3. This low-energy asymmetry of the SW resemble that obtained in CF metals occurring in single layers at $\nu = 1/2$ [20]. Similar SF_{CF} modes are observed at $\nu_T < 1$ and disappear as the total filling factor approaches the QH state at $\nu_T = 2/3$.

These results demonstrate the emergence of a CF metal phase in compressible electron bilayers at $\nu_T = 1$. Analysis of the energy onset of the SF_{CF} continuum (the spin-gap E_{gap}^{CF} of the bilayer CF metal) raises the possibility that full spin polarization of the CF metal is lost at a rather-low critical value of the ratio $\xi = E_z/E_c$. ξ measures of the impact of spin in Coulomb interactions linked to formation of CF quasiparticles and highlights the role played by the spin degree of freedom in quantum phases of bilayers close to $\nu_T = 1$.

Such studies of low-lying spin excitations by light scattering methods offer venues to study the multiplicity of states that can occur near the compressible-incompressible phase boundary at $\nu_T = 1$ [3, 8, 10, 11, 12, 13, 14, 15]. The observations of CF ground states at low values of Δ_{SAS}/E_c and of excitonic states at larger Δ_{SAS}/E_c suggests a subtle competition between these correlated electronic phases near the phase transition. [21].

Experiments were carried out in two nominally symmetric modulation-doped $Al_{0.1}Ga_{0.9}As/GaAs$ double quantum wells (DQWs) grown by molecular beam epitaxy and having total electron densities of $n \sim 1.1 - 1.2 \times 10^{11}$ cm^{-2}, mobilities above 10^6 cm^2/Vs and Δ_{SAS} of 0.36 meV (sample A) and 0.1 meV (sample C). Resonant inelastic light scattering was performed on samples in a dilution refrigerator with a base temperature of ~ 50 mK. A tilted angle geometry with a tilt angle θ between the total applied magnetic field (B_T) and the direction perpendicular to the sample surface was exploited. The non-zero tilt angle gives access to spin excitations when the incident and scattered photons have crossed polarizations. It also leads to non-zero components of the in-plane magnetic field that allows to tune Δ_{SAS} [6, 18]. Measurements were performed with laser power densities of $10^{-3} - 10^{-4}$ W/cm^2 with a titanium-sapphire laser tuned close to the DQW optical gap.

Figure 1(a) shows the calculated position of the two samples at the investigated tilt angles in the $\nu_T = 1$ phase diagram of compressible (NO QH) and incompressible (QH) phases. At sufficiently low values of the inter-layer coupling ($d/l_B \to \infty$, $\Delta_{SAS}/E_c \to 0$) the ground state can be understood as composed of CF metals in each of the two layers at $\nu = 1/2$, as shown in Fig.1(b). This state is characterized by a CF Fermi level E_F and a CF spin-gap E_{gap}^{CF} that separates the highest occupied CF level with spin-up from the lowest unoccupied CF level with spin-down. Figure 1(b) refers to the case $E_{gap}^{CF} > 0$ that corresponds to a fully spin polarized CF metal.

Spin excitation spectra in the $\nu_T = 1$ compressible phase are displayed in Figs. 2(a-c) for sample A at three different angles θ. The spectra manifest low-energy SF_{CF} excitations (green regions) in addition to the long-wavelength SW peak centered at E_z due to the Larmor theorem. The SW peak are modeled by a gaussian line centered at E_z and with a broadening of 30 μeV. Additional high-energy scattering (in orange) arises because breakdown of wavevector conservation couples the light to high-energy SW modes at finite wavevectors. The low-energy scattering is due to spin excitations because it displays light scattering selection rules identical to the SW peak. The SF_{CF} feature is assigned to the continuum of CF spin excitations as suggested by the schematic drawing of CF energy levels with CF filling factor $\nu_{CF} = \infty$ (where $\nu = \nu_{CF}/(2\nu_{CF} \pm 1)$), and spin transitions shown in the right-bottom part of Fig. 3 [20]. For $\theta = 45^o$ and 52.5^o the SF_{CF} continuum stops at finite values of E_{gap}^{CF}. For $\theta = 35^o$ the continuum extends below the lowest accessible energy of 30 μeV given by the laser stray light which we take as an indication that the CF metal develops a tendency to lose its spin polarization at this angle. In order to extract quantitative information on SF_{CF} continuum and E_{gap}^{CF} the background signal due to the laser tail and magneto-luminescence was carefully evaluated. The background (dashed line) is shown in Figs. 2(a-c) and Fig. 3 for sample A and C, respectively. The same procedure was adopted for the spectra in the

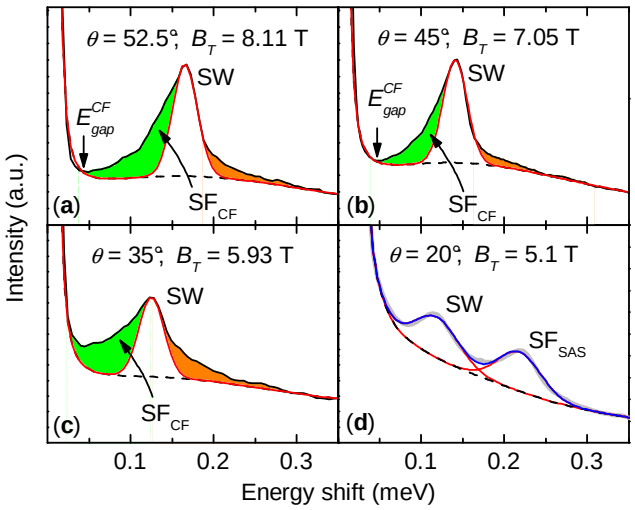

FIG. 2: $(a-c)$ Resonant inelastic light scattering spectra of long-wavelength spin wave (SW) (gaussian line in red) and composite-fermion spin-flip SF_{CF} modes (green area) at ν_T = 1 and T = 60mK for different values of tilt angle θ. Dashed line represents the background due to laser tail and magneto-luminescence. High-energy scattering (orange area) due to disorder-activated SWs at finite wave-vectors is also shown. For $\theta = 52.5^o$ (a) and 45^o (b) the SF_{CF} continuum (green areas) stops at E_{gap}^{CF} that represents the spin-gap for CF spin excitations across the Fermi energy (see Fig.1). At $\theta = 35^o$ the continuum extends at energies below the laser stray light. (d) SW and intersubband spin-flip (SF_{SAS}) modes in the quantum Hall phase at $\theta = 20^o$. Red lines are gaussian fits to the SW and SF_{SAS}. Blue line is the fit to the spectrum including the background signal (dashed line). Lorentzian fits of the SW peaks (not shown) lead to similar evaluations of the SF_{CF} continuum and E_{gap}^{CF}.

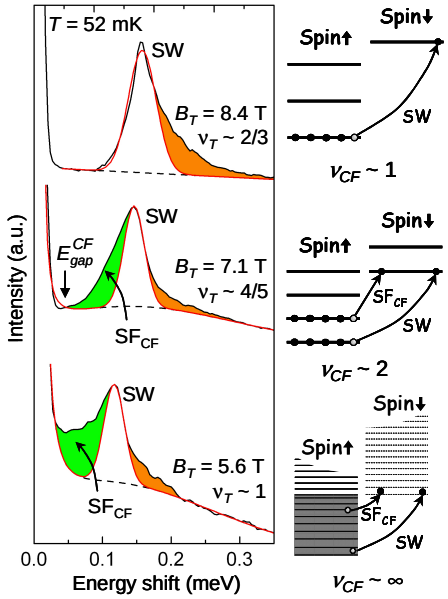

FIG. 3: (Left) Spin excitation spectra at three different values of ν_T for sample C at a tilt angle of $\theta = 30^o$. The notations are the same used in Fig.2. The green area that represents the spin-reversal SF_{CF} continuum disappears at $\nu_T = 2/3$ when one spin-up CF Landau level is expected to be occupied. (Right) Representation of composite-fermion (CF) energy levels. Expected occupation of CF quasiparticles and CF filling factor ν_{CF} are presented for $\nu_T = 2/3$ and 4/5 and 1. SW and the low-lying SF_{CF} modes are also shown.

incompressible phase (Fig. 2(d)).

Below the critical angle $\theta = 35^o$, the SF_{CF} continuum disappears and a well-defined intersubband spin-flip SF_{SAS} mode across the tunneling gap is observed as shown in Fig.2(d). Mean-field approaches predict that the SW-SF_{SAS} energy splitting should be equal to Δ_{SAS}. Our previous work [6], on the contrary, has shown that the splitting is instead less than Δ_{SAS} and determined by the density of excitonic electron-hole pairs that exist across Δ_{SAS}. These excitonic states are induced by the inter-layer correlations in the incompressible QH phase [22]. The phase transition is seen at the collapse of the SW-SF_{SAS} splitting when the excitonic density reaches half of the electron density [6]. The results reported here show that the transition is associated with the appearence of low lying SF_{CF} excitations which demonstrates that close to the critical angle there is a crossover from an excitonic QH state to a CF metal. Remarkably enough, the inelastic light scattering measurements reveal that even very close to the phase boundary, the compressible state shows characteristic manifestations of CF quasiparticles despite the residual impact of inter-layer interactions.

Figure 3 reports representative spectra of spin excitations at three different values of ν_T =1, 4/5 and 2/3 in sample C. The right part of Fig.3 shows the corresponding CF energy level schemes, occupations and CF filling fraction ν_{CF}. Similar to what is reported in Figs 2(a-c) for sample A, the spectral line shape at $\nu_T = 1$ shown in Fig.3 is largely affected by SF_{CF} modes that are signatures of the double-layer CF metal. The low-lying continuum of SF_{CF} excitations at $\nu_T = 1$ (green region) extends below the lowest accessible energy signaling possible loss of spin polarization. At $\nu_T \sim 4/5$, instead, the E_{gap}^{CF} becomes finite demonstrating that at this magnetic field the system has full spin polarization.

The assignment of the low-energy scattering to spin excitations of the CF metal is confirmed by the observation that it disappears when approaching the QH state at $\nu_T = 2/3$. In this regime the bilayer is composed of two weakly-coupled incompressible $\nu = 1/3$ QH states in which only the lowest spin-up CF level is occupied (upper-right part of Fig. 3). No low-lying SF_{CF} excitations can exist in this case consistent with the SW lineshape shown in Fig.3. The observed SW peak at $\nu_T = 2/3$ is indeed largely asymmetric only at high energy (orange area) as expected for a weakly-disordered

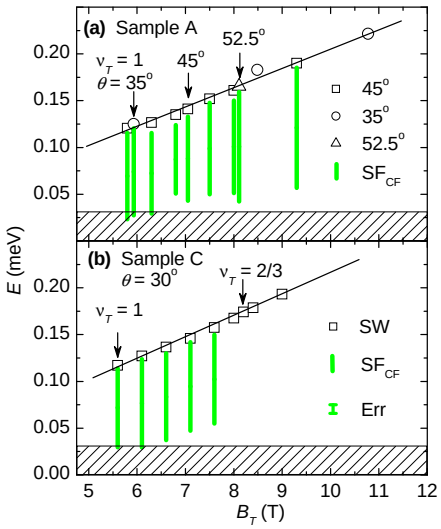

FIG. 4: Energies of low-lying spin excitations as a function of total magnetic field in sample A at different angles (a) and in sample C (b). Vertical green bars correspond to the contribution of the composite-fermion SF_{CF} excitations. Open symbols correspond to the long wavelength limit of the SW. Solid line is a fit with the relation $E_z = |g_e|\mu_B B$ yielding $|g_e| = 0.41$. Shaded region at low energy represents the energy range of ~ 30 μeV not accessible in our experiments due to the laser tail. Typical error bar (Err) in the evaluation of the continuum obtained by comparing results with Gaussian and Lorentzian lineshapes for the SW is also shown.

QH state

Figure 4 describes the evolution of the SW peak energy (open dots) and the extension of the SF_{CF} continuum (vertical bars) in samples A and C. The angles are chosen such that $\nu_T = 1$ corresponds always to the compressible phase (see Fig. 1(a)). In sample A the E_{gap}^{CF} at $\nu_T = 1$ remains nearly constant at higher angles ($> 45^o$) and becomes lower than our experimental uncertainty between the values of 45^o and 35^o suggesting a tendency of the CF metal to lose its spin polarization at low values of E_z.

We note that E_{gap}^{CF} is given by the difference between the energy required to flip a single CF spin and the Fermi energy of the CF sea, i.e. $E_z + E^{\uparrow\downarrow} - E_F^{CF} = E_{gap}^{CF}$, where $E^{\uparrow\downarrow}$ arises from the residual interactions among CFs [23]. Both $E^{\uparrow\downarrow}$ and E_F^{CF} scales with E_c and therefore depends on the perpendicular component of the magnetic field, while E_z depends on the total magnetic field. We can thus estimate an upper value of the critical value of $\xi = E_z/E_c$ separating fully spin-polarized from partially spin-polarized bilayer CF metals. We obtain $\xi_c \leq 0.013 \pm 0.001$ in sample A. This is lower than the value of $\xi_c \approx 0.017$ found in single-layer CF metals with similar densities [23]. In a simplified framework, this result can be understood by invoking a CF effective mass larger than the value of $\approx 0.4 m_o$ found in single layers (m_o is the free electron mass) [20]. The larger mass may originate from the impact of inter-layer interactions or reflect the higher disorder of double layers.

Figure 4(b) highlights that the SF_{CF} continuum in sample C disappears above $B_T = 8$ T (close to $\nu_T = 2/3$) as also shown in Fig.3. Additionally the E_{gap}^{CF} becomes lower than the experimental uncertainty for magnetic fields below 6T ($E_z \approx 0.13$meV) suggesting loss of spin polarization in this range of magnetic fields consistent with data obtained in sample A.

In conclusion, light scattering spectra uncovered a phase transformation of an excitonic incompressible state into a compressible (metallic) CF phase as the tunneling gap collapses in electron bilayers at ν_T =1. Studies of the CF metal near the compressible-incompressible phase boundary could offer insights on interactions involved in the emergence of ground states due the impact of inter- and intra-layer correlations in electron bilayers in the quantum Hall regimes.

We are grateful to Steven H. Simon for useful comments. VP acknowledges the Italian Ministry of Research (FIRB). AP acknowledges the National Science Foundation under Award Number DMR-03-52738, the Department of Energy under award DE-AIO2-04ER46133, and the W. M. Keck Foundation.

[1] S.M. Girvin, A.H. MacDonald, in *Perspectives in quantum Hall effects* , edited by S. Das Sarma and A. Pinczuk (Wiley, New York 1997), Chap. 5 p.161.
[2] G.S. Boebinger et al., Phys. Rev. Lett. **64**, 1793 (1990); S.Q. Murphy et al., Phys. Rev. Lett. **72**, 728 (1994).
[3] S.H. Simon et al., Phys. Rev. Lett. **91**, 046803 (2003).
[4] M. Kellogg et al., Phys. Rev. Lett. **93**, 036801 (2004).
[5] A.H. MacDonald, P.M. Platzman, G.S. Boebinger, Phys. Rev. Lett. 65, 775 (1990); L. Brey, Phys. Rev. Lett. **65**, 903 (1989).
[6] S. Luin, et al., Phys. Rev. Lett. **94**, 146804 (2005).
[7] S. Luin et al., Phys. Rev. Lett. **90**, 236802 (2003).
[8] D.N. Sheng et al., Phys. Rev. Lett. **91**, 116802 (2003).
[9] J.K. Jain, Phys. Rev. Lett. **63**, 199 (1989).
[10] A. Stern, and B.I. Halperin, Phys. Rev. Lett. **88**, 106801 (2002).
[11] N.E. Bonesteel et al., Phys. Rev. Lett. **77**, 3009 (1996).
[12] J. Schliemann et al., Phys. Rev. Lett. **86**, 1849 (2001).
[13] Y.B. Kim et al., Phys. Rev. B **63**, 205315 (2001).
[14] M.Y. Veillette et al., Phys. Rev. B **66**, 155401 (2002).
[15] E. Demler et al., Phys. Rev. Lett. **86**, 1853 (2001).
[16] I.B. Spielman, et al., Phys. Rev. Lett. **94** 076803 (2005).
[17] N. Kumada, et al., Phys. Rev. Lett. **94** 096802 (2005).
[18] J. Hu, and A.H. MacDonald, Phys. Rev. B **46**, 12554 (1992).
[19] S.S. Mandal and J.K. Jain, Phys. Rev. B **63**, 210310 (2001).
[20] I. Dujovne et al., Phys. Rev. Lett. **90**, 036803 (2003).
[21] S. Luin et al., Phys. Rev. Lett. **97**, 216802 (2006).
[22] M. Polini, et al., Solid State Comm. **135**, 654 (2005).
[23] I. Dujovne et al., Phys. Rev. Lett. **95**, 056808 (2005).